Decreasing *LTP2* expression increases phenotypic variation in early seedling traits of *Arabidopsis thaliana*

Cristina M Alexandre[1], Kerry L Bubb[1], Karla M Schultz[1], Janne Lempe[2], Josh T Cuperus[1,*] and Christine Queitsch [1,3,*]

Affiliations:
1: Department of Genome Sciences, University of Washington, Seattle WA 98195, USA.
2: Julius Kühn Institute (JKI) - Federal Research Centre for Cultivated Plants, Institute for Breeding Research on Fruit Crops, Dresden, Germany.
3: Brotman Baty Institute for Precision Medicine, Seattle, WA 98195, USA
*:Corresponding Authors,
Cuperusj@uw.edu
Quietsch@uw.edu

ABSTRACT

Isogenic individuals can display seemingly stochastic phenotypic differences, limiting the accuracy of genotype-to-phenotype predictions. The extent of this phenotypic variation depends in part on genetic background, raising questions about the genes involved in controlling stochastic phenotypic variation. Focusing on early seedling traits in *Arabidopsis thaliana*, we found that hypomorphs of the cuticle-related gene *LTP2* greatly increased variation in seedling phenotypes, including hypocotyl length, gravitropism and cuticle permeability. Many *ltp2* hypocotyls were significantly shorter than wild-type hypocotyls while others resembled the wild type. Differences in epidermal properties and gene expression between *ltp2* seedlings with long and short hypocotyls suggest a loss of cuticle integrity as the primary determinant of the observed phenotypic variation. We identified environmental conditions that reveal or mask the increased variation in *ltp2* hypomorphs, and found that increased expression of its closest paralog *LTP1* is necessary for *ltp2* phenotypes. Our results illustrate how decreased expression of a single gene can generate starkly increased phenotypic variation in isogenic individuals in response to an environmental challenge.

Keywords hypocotyl; lipid transfer protein; *LTP2*; cuticle integrity; non-genetic variation; phenotypic variation; stochasticity; phenotypic robustness, hypomorph; gene-by-environment interaction

INTRODUCTION

Genetically identical individuals can develop different phenotypes. Understanding the mechanistic underpinnings of this non-genetic phenotypic variation and the relative contributions of environmental factors and stochasticity holds promise for more accurate genotype-phenotype predictions. As early as 1920, Sewall Wright wrote that a sizable fraction of the environmental contribution to phenotypic variation is likely missed experimentally, and suggested that stochasticity may play an important role in shaping individual phenotypes (Wright 1920). Individuals sampled from an isogenic population can differ because of (1) stochastic differences

in gene expression (Elowitz et al. 2002; Blake et al. 2003; Raser and O'Shea 2004; Lomvardas et al. 2006; Volfson et al. 2006; Gimelbrant et al. 2007), protein levels (Feinerman et al. 2008) or metabolic states (Smith et al. 2007; van Heerden et al. 2014); (2) parental effects (Perez et al. 2017); or (3) differences in microenvironments, relative position or other contextual information (Eagle and Levine 1967; Snijder et al. 2009). None of these possible causes are mutually exclusive. Even subtle differences can have large cumulative effects, because the internal state of individuals affects how they respond to environment factors. A classic example of environmentally-induced heterogeneity is the behavior of a collection of temperature-sensitive cell-cycle mutants in yeast. When grown asynchronously, these mutants show heterogeneous, non-heritable phenotypes due to individual cells experiencing the restrictive temperature treatment at different stages in the cell cycle (Hartwell et al. 1974). A multitude of studies in animals and plants have shown that the extent of non-genetic phenotypic variation across individuals and populations depends in part on genotype, with some genetic backgrounds of the same species showing greater non-genetic variation (or less phenotypic robustness) than others (Waddington 1942; Whitlock and Fowler 1999; Ros et al. 2004; Hall et al. 2007; Hill et al. 2007; Ansel et al. 2008; Sangster et al. 2008; Shen et al. 2012; Ayroles et al. 2015; Morgante et al. 2015; Katsanos et al. 2017).

The more that increased, non-genetic phenotypic variation occurs in a particular genetic background, the lower will be our ability to predict phenotype from genotype, because the same genetic variants will show different expressivity in different individuals (Eldar et al. 2009; Raj et al. 2010; Burga et al. 2011; Casanueva et al. 2012; Queitsch et al. 2012, 2002; Zabinsky et al. 2019; Lachowiec et al. 2016). Therefore, non-genetic phenotypic variation has wide-ranging implications, from cancer drug resistance (Sharma et al. 2010; Márquez-Jurado et al. 2018; Emert et al. 2021; Shaffer et al. 2017) to microbial bioproduction (Delvigne et al. 2014; Xiao et al. 2016). In agriculture, trait uniformity is particularly highly prized (Finch-Savage and Bassel 2016; Tran et al. 2017), and breeding programs rely on parental performance. A better understanding of the genetic underpinnings of non-genetic phenotypic variation and their interplay with environmental factors might inform targeted breeding of more robustly performing varieties. In plants, several genes have been identified that affect non-genetic variation of traits like growth (Joseph et al. 2015; Illouz-Eliaz et al. 2019), organ size or number (Hall et al. 2007; Hong et al. 2016), germination (Abley et al. 2021), early seedling phenotypes (Queitsch et al. 2002; Lemus et al. 2023; Mason et al. 2016; Lachowiec et al. 2018) and defense metabolites (Joseph et al. 2015; Jimenez-Gomez et al. 2011).

Here, we focus on hypocotyl elongation in the dark, an adaptive trait relevant for seedling establishment. Hypocotyl elongation in the dark shows large non-genetic variation in *A. thaliana* (~10% coefficient of variation in hypocotyl length(Borevitz et al. 2002; Maloof et al. 2001; Sangster et al. 2008; Lachowiec et al. 2018; Queitsch et al. 2002). We found that hypomorphs of *LTP2* (*LIPID TRANSFER PROTEIN 2*/AT2G38530), a highly expressed gene in dark-grown seedlings, show increased phenotypic variation under specific environmental conditions. Plant Lipid Transfer Proteins (LTPs) are a family of small (~9 kDa) lipid-binding, cysteine-rich proteins that are commonly found in the shoot epidermis (Kader 1996; Yeats and Rose 2008). While structurally similar, LTPs have different expression patterns, suggesting functional specialization (Arondel12 et al. 2000; Chae et al. 2010). LTPs have been associated with antimicrobial activity

and cuticle physiology, and are implicated in a wide variety of biological processes (Finkina et al. 2016; Nieuwland et al. 2005; Cameron et al. 2006; Potocka et al. 2012; Molina et al. 1993; Buhot et al. 2001; Chae et al. 2010; Maldonado et al. 2002; Gao et al. 2016; Debono et al. 2009; Chae et al. 2009).

LTP2 is abundant in the epidermal cell wall of dark-grown hypocotyls (Jacq et al. 2017; Irshad et al. 2008), where it promotes cuticle integrity and desiccation tolerance (Jacq et al. 2017). We found that under certain environmental conditions, *LTP2* is necessary for full hypocotyl elongation in the dark, and that a decrease in *LTP2* expression increases variation in hypocotyl length, gravitropism and cuticle permeability in isogenic seedlings. Differences in epidermal morphology and cuticle permeability between long and short *ltp2* hypocotyls and between growth conditions that promote or mask trait variation suggest that loss of cuticle integrity in *ltp2* hypocotyls is the main determinant of this background's increased non-genetic phenotypic variation.

RESULTS

Decreased *LTP2* expression increases non-genetic phenotypic variation in skotomorphogenesis

Young seedlings grown in the dark show common skotomorphogenic phenotypes with elongated hypocotyls, etiolated cotyledons and short roots (Vandenbussche et al. 2005; Gendreau et al. 1997). *LTP2* is among the most highly expressed genes in dark-grown shoots (99th percentile, Figure S1A, B), suggesting that its function is required during skotomorphogenesis. To measure the impact of *LTP2* on the phenotypic variation of elongating hypocotyls, we used two *ltp2* hypomorphs, *ltp2-1* and *ltp2-2,* harboring T-DNA insertions less than 500 bp upstream of the *LTP2* transcriptional start site (Figure 1A). Both lines expressed less than 25% of wild-type *LTP2* RNA levels in dark-grown shoots (Figure 1B), and showed similar defects in skotomorphogenesis. When grown in the dark, *ltp2* hypocotyls were shorter (Figure 1C, D) and more variable than wild type (Col-0; Figure 1C), in both length (Figure 1E) and orientation (Figure 1F). Hypocotyl lengths were almost twice as variable in *ltp2-1* as in Col-0 wild type (merged coefficient of variation, CV, of 21% *vs* 13%), with *ltp2-2* being slightly less variable (merged CV 18%; Figure 1E). The higher variation in the hypomorphs was not due to a bimodal distribution but to a continuous, wider distribution of hypocotyl lengths (Figure 1D). An even larger difference was measured for hypocotyl orientation (CV 34-37% *vs* 10%; Figure 1F), a proxy for reduced negative gravitropism. However, there was no significant correlation between hypocotyl length and orientation of individual seedlings (Figure S1C). Consistent with a non-genetic origin for this increased variation in hypocotyl length, the selfed offspring of *ltp2* parents with either long or short hypocotyls showed similar mean hypocotyl lengths (Figure 1G). Other notable *ltp2* phenotypes included longer roots than hypocotyls, resulting in a smaller hypocotyl/root ratio per individual seedling than in Col-0 wild type (Figure 1H), and a tendency for expanded cotyledons (Figure 1C arrowhead, 1I). Taken together, reduced levels of *LTP2* globally affect non-genetic variation in skotomorphogenesis.

ltp2 phenotypes show strong gene-by-environment interaction

Next, we explored internal and external factors that might be associated with the hypocotyl length of individual seedlings or modulate the extent of phenotypic variation in *ltp2* hypomorphs. We started by examining the influence of seed batch, seed germination and seed size on hypocotyl length. We found similar mean hypocotyl lengths (Figure S2A) and similarly high coefficients of variation with different *ltp2* seed batches (Figure 1E). There was no germination delay or increased heterogeneity in germination in the *ltp2* hypomorphs relative to Col-0 wild type, as inferred from the correlation of hypocotyl and root length and its time-dependent drop in seedling development (Figure S2B). Finally, hypocotyl length of individual seedlings was not explained by seed size in either the *ltp2* hypomorphs or Col-0 wild type (Figure S2C).

We continued by examining the impact of the growth medium. In the dark, hypocotyls grow longer if provided with sucrose. However, the presence of sucrose also modifies hypocotyl and root growth kinetics (Kircher and Schopfer 2012)(Figure S3A) and is associated with a decrease in the hypocotyl/root ratio compared to growth conditions without sucrose (Kircher and Schopfer 2012) (Figure S3B). We reasoned that the presence of sucrose might affect variation in hypocotyl elongation. In our typical experimental setup, hypocotyls grow in direct contact with the medium, and sucrose-driven hypocotyl elongation depends on shoot uptake, although not necessarily via hypocotyls (Figure S3C). A comparison between *ltp2* seedlings grown on MS media, MS+1% sucrose or MS+1% glucose revealed that *ltp2* phenotypes were strongly sucrose-dependent. Either removing sucrose or replacing it with glucose was sufficient to rescue all *ltp2* growth phenotypes, including differences in mean length and coefficient of variation (Figure 2A,B), hypocotyl negative gravitropism (Figure 2C and hypocotyl/root ratio (Figure 2D). Therefore, *ltp2* hypocotyls can fully elongate under favorable conditions. Sucrose did not cause an increase in the coefficient of variation of hypocotyl length in wild type Col-0, despite a noticeable increase in mean length in this condition (Figure 2A-B).

<u>A sucrose-dependent increase in cuticle permeability is associated with short *ltp2* hypocotyls</u>

A comparison of *ltp2* hypocotyls grown with and without sucrose revealed epidermal features that were associated with short hypocotyls. Compared to wild-type Col-0, the epidermal surface of *ltp2* hypocotyls was not smooth, and instead was fuzzy or wrinkled (Figure 2E); this *ltp2* phenotype was sucrose-specific and much stronger in short than in long *ltp2* hypocotyls (Figure 2E). Furthermore, growth with sucrose greatly increased permeability to the water-soluble dye toluidine blue, an indicator of cuticle integrity (Tanaka et al. 2004), in *ltp2* hypocotyls, but not in Col-0 hypocotyls, compared to controls without sucrose. Most *ltp2* hypocotyls stained deeply, and over more than 50% of their full length (Figure 2F-G), consistent with reduced cuticle integrity (Jacq et al. 2017). The extent of staining varied widely in *ltp2* hypocotyls, from 0 to 100% (Figure 2G). On average, heavily stained hypocotyls were smaller than those not stained (Figure 2G), and *ltp2* seedlings with the wild-type-like hypocotyl/root ratio > 1 were less stained overall (Figure 2G). In contrast, staining in Col-0 wild-type hypocotyls was generally weak and spatially restricted (Figure 2F-G). These results suggest that altered cuticle integrity contributes to the sucrose-dependent inhibition of hypocotyl elongation in *ltp2* seedlings.

<u>Hypocotyl length is associated with many transcriptional differences in *ltp2* seedlings</u>

To identify what molecular functions are associated with non-genetic variation in hypocotyl length, we compared the transcriptional profiles of Col-0 and *ltp2* seedlings with short (S) and long (L) hypocotyls (bottom and top 15th percentiles, respectively; Figure 3A). For each genotype by length combination, we performed bulk RNA-seq on two replicate pools of 70 shoots each (Figure 3A; see Figure S4A-C for QC metrics). Principal component analysis indicated that *ltp2* samples with short and long hypocotyls were distinguishable by their global expression patterns, whereas wild-type pools were not (Figure 3B). Nearly half of the global variance in gene expression (47%, PC1) was correlated with mean hypocotyl length (Figure 3C). Over 20 times as many differentially expressed genes (DEGs, log2FC >=1 and p-adj < 0.01) were found between the short and long *ltp2* samples (584, Table S2) compared to the Col-0 samples (24, Table S1). The differentially expressed genes associated with hypocotyl length in *ltp2* samples were enriched in gene ontology (GO) terms related to cell wall modification, response to stress and plant defense (Figure 3D, fold-enrichment >= 2, p-adj < 0.05). *ltp2* samples with short hypocotyls showed downregulation of cell wall-related genes that promote growth, like *PGX1* and *XTH20* (Miedes et al. 2013; Xiao et al. 2014), secondary cell wall biosynthesis genes, including the three main laccases *LAC4*, *LAC11* and *LAC17,* and several peroxidases and genes related to casparian strip deposition (Figure 3E). Although casparian strip biology is not well studied outside of roots, the casparian strip is present in dark-grown hypocotyls (Karahara 2012; Geldner 2013). None of the genes in the enriched term “casparian strip” were differentially expressed between Col-0 wild-type and *ltp2* seedlings with long hypocotyls (Figure 3E), suggesting that the down-regulation of these genes may contribute to the phenotype of *ltp2* seedlings with short hypocotyls.

We also observed the upregulation of a variety of stress and defense-response genes related to hypoxia, response to fungus, anthocyanin and jasmonate biosynthesis (Figure 3F). A few of these genes (10), including several of the most highly upregulated genes in *ltp2* seedlings with short hypocotyls, were also upregulated in Col-0 seedlings with short hypocotyls compared to Col-0 seedlings with long hypocotyls (Figure S4D-E). This result supports the idea that the phenotypic impact of perceived stress on hypocotyl length for a given individual can be genotype-independent; however, *ltp2* individuals experience this impact far more frequently and far more severely.

The majority of the differentially expressed genes (474, 81%) between the long and short *ltp2* samples were also differentially expressed between the short samples of *ltp2* and Col-0. This result likely reflects that difference in mean hypocotyl length between the short *ltp2* and the short wild-type samples is about as large as the difference between the long and the short *ltp2* samples (Figure S4A). However, we found more than twice as many differentially expressed genes (1638) in the comparison of the short *ltp2* and short wild-type samples (Figure S4G). These differentially expressed genes showed similar gene ontology enrichments as found for the comparison of long and short *ltp2* samples, related to hypoxia, oxidative stress, plant defense and cell wall metabolism, with additional growth-related terms such as response to auxin (Figure S4H). Indeed, we found that many auxin-responsive genes, including some with known roles in hypocotyl elongation and/or gravitropism like *SAUR19/23/24/32* (Spartz et al. 2012; Park et al. 2007), *ARGOS* (Rai et al. 2015), *SHY2* (Tian et al. 2002; Reed et al. 1998) and *HAT2* (Sawa et al. 2002), were downregulated in *ltp2* seedlings with short hypocotyls compared

to wild-type seedlings with short hypocotyls, but not compared to *ltp2* seedlings with long hypocotyls (Table S5). Most of the differentially expressed genes in the short sample comparison (996/1164, 86%) did not overlap with the differentially expressed genes in the long sample comparison. Because the *ltp2* seedlings with long hypocotyls and Col-0 wild-type seedlings with long hypocotyls differ in genotype but little in mean hypocotyl length, we conclude that the gene expression differences across samples are strongly associated with hypocotyl length, in particular with the strongly reduced hypocotyl length of short *ltp2* seedlings.

ltp2 phenotypes depend on upregulation of its closest paralog *LTP1*

Focusing on cuticle-related genes (see Methods; from (Li-Beisson et al. 2013), we found that 21 out of the 160 expressed in dark-grown shoots were deregulated in *ltp2* relative to Col-0 seedlings (30% more than expected, p=0.019; Table S6). Most of these genes (19/21) were upregulated in *ltp2*, including six other LTP paralogs (Figure 4A). To explore to what extent close paralogs may compensate for reduced *LTP2* expression, we examined the role of its nearest paralog, *LTP1* (Figure 4B, Figure S5A). Analysis of *LTP1* and *LTP2* expression in light- and dark-grown wild-type seedlings showed a reciprocal expression pattern that suggests non-redundant roles during hypocotyl elongation: whereas *LTP1* was about 100 times more abundant than *LTP2* in the light, it was 1/10 times as abundant in the dark (Figure 4C). In dark-grown seedlings, *LTP2* accounts for more than 86% of global Type I LTP expression compared to only 5% for *LTP1* (Figure S5B). In stark contrast, *LTP1* tends to be the more abundantly expressed paralog in many other conditions, organs, and developmental stages (41/56 samples; Figure S5C). Moreover, we found that *LTP1* expression was no longer repressed in the dark in *ltp2* seedlings, nearly reaching levels found in light-grown seedlings (Figure 4C, Figure 5SB). We wondered whether *LTP1* upregulation and the altered expression ratio of the paralogs might contribute to the *ltp2* phenotypes. To test this hypothesis, we used an artificial microRNA to simultaneously knock-down *LTP1* and *LTP2* gene expression while aiming for a similar *LTP1*/*LTP2* ratio as found in Col-0 wild-type (Figure 4D). Remarkably, the mean value and variation of hypocotyl length of the *ltp1 ltp2* double knock-down seedlings closely resembled those of Col-0 wild-type seedlings with both distributions largely overlapping (Figure 4E, F). The *ltp1 ltp2* double knock-down seedlings were also similar to Col-0 wild-type seedlings in hypocotyl/root ratio (Figure 4G) and hypocotyl cuticle integrity (Figure 4H). We conclude that the upregulation of *LTP1* compared to low expression levels of *LTP2* in dark-grown seedlings contributes to the variable skotomorphogenesis phenotypes of the *ltp2* hypomorphs (Figure S5D, E) whereas the repression of *LTP1* compared to high levels of *LTP2* contributes to the long, relatively uniform hypocotyls of dark-grown wild-type- seedlings.

DISCUSSION

Here, we show that the gene *LTP2* plays an important role in shaping skotomorphogenesis traits. Hypomorphs of *LTP2* show increased phenotypic variation in three hypocotyl traits: negative gravitropism, length and cuticle permeability. For the latter two, the increased variation was accompanied by altered mean values relative to wild type, with most *ltp2* dark-grown

seedlings having short hypocotyls with highly permeable cuticles. Variation in hypocotyl length increases in dark-grown hypocotyls upon perturbation of the chaperone Hsp90 (Queitsch et al. 2002; Sangster et al. 2008), or its client protein BEH4 (Lachowiec et al. 2018), as well as in *AGO1* hypomorphs (Lemus et al. 2023). As for the *ltp2* hypomorphs described here, in these three cases, the increased variation in hypocotyl length was also accompanied by decreased length means. This concordance of changes in mean and variation might be expected if wild-type hypocotyls reach lengths close to their maximum physiological limit under these experimental conditions.

In *ltp2* hypocotyls, a strong defect in cuticle permeability was associated with reduced elongation and increased phenotypic variation compared to wild type; however, these phenotypes depended on exposure to sucrose. This remarkably strong gene-by-environment effect is unlikely due to a higher requirement for LTP2 function, as hypocotyls elongate more when provided with an exogenous carbon source. *LTP2* is required in dark-grown hypocotyls to seal the cuticle and prevent water loss (Jacq et al. 2017). Moreover, increased cuticle permeability is linked to structural defects and poor adhesion between the cuticle and the rest of the cell wall. Our finding that *ltp2* hypocotyls were much more susceptible to sucrose-induced dye uptake than wild type is consistent with *LTP2*'s role in cuticle sealing and suggests that sucrose acts as a cuticle stress. Sucrose may trigger gene expression changes that modify cuticle composition or act directly to increase cuticle hydration, the mechanical strain associated with water accumulating in the cuticle and in gaps between the cuticle and the cell wall. This added strain could lead to further cuticle detachment in sensitized *ltp2* hypocotyls, thus aggravating their documented cuticle integrity defect (Jacq et al. 2017). The sucrose-induced loss of cuticle integrity is likely the primary determinant of the shorter *ltp2* hypocotyls and their increased variation in length.

Dark-grown long hypocotyls have thick cuticles (Gendreau et al. 1997), and shorter hypocotyls are associated with pharmacological or genetic disruptions in cuticular wax biosynthesis and deposition (Narukawa et al. 2016). The greater need for cuticle integrity during hypocotyl elongation in the dark may reflect a seedling's push upwards through the soil while minimizing abrasion and the need for structural reinforcement due to cell wall thinning in very long cells (Derbyshire et al. 2007). Loss of cuticle barrier function causes water loss and activates cuticle-dependent defense priming (Bessire et al. 2007; Chassot et al. 2007; Serrano et al. 2014; L'Haridon et al. 2011), which inhibits growth, and is consistent with the gene ontology enrichments observed among upregulated genes in *ltp2* seedlings with short hypocotyls compared to those with long ones. However, the precise mechanisms by which *LPT2* facilitates the elongation of dark-grown hypocotyls remain unknown.

In contrast to phenotypic buffers, which act on gene regulation (Lachowiec et al. 2018, 2016; Lemus et al. 2023) or protein folding (Queitsch et al. 2002; Sangster et al. 2008; Zabinsky et al. 2019; Lachowiec et al. 2016), *LTP2* appears to act structurally by sealing the cuticle. The integrity of this seal determines the effectiveness of the cuticle as an insulating barrier, thus providing a simple mechanism of phenotypic robustness against environmental insults. Biophysical and regulatory complexity makes plant cuticles liable to harbor considerable non-

genetic variation in their composition, ultra-structure and properties, in particular when considering the complexity of the environments plants face. Upon damage or genetic perturbation, this intrinsic variation is amplified as shown by the disorganized cuticles of mutants with cutin defects or increased cuticle permeability (Chen et al. 2003; Kurdyukov et al. 2006; Lolle et al. 1992; Schnurr et al. 2004; Wellesen et al. 2001; Sieber et al. 2000; Takahashi et al. 2010).

Loss of cuticle integrity may not fully explain the increased phenotypic variation of *ltp2* seedlings. We cannot rule out that the increased phenotypic variation depends on another, yet undiscovered *LTP2*- function. However, our results that show genetic interactions between the close paralogs *LTP1* and *LTP2*, and that their expression ratio is a determinant of increased cuticle permeability and phenotypic variation during skotomorphogenesis, strongly support our interpretation. In crown gall tumors, the only other context outside of skotomorphogenesis where *ltp2* phenotypes have been identified (Jacq et al. 2017), *LTP1* is also highly upregulated (Deeken et al. 2016). This finding is consistent with our result that the upregulation of *LTP1* compared to *LTP2* expression is predictive of the deleterious *ltp2* phenotypes.

While paralogs with redundant or partially redundant functions can confer genetic robustness (Gu et al. 2003; Kafri et al. 2005; Dean et al. 2008; DeLuna et al. 2010; Diss et al. 2014; DeLuna et al. 2008), this is not universally observed (Ihmels et al. 2007; Dandage and Landry 2019; DeLuna et al. 2010; Diss et al. 2017). In fact, incomplete functional compensation can be a source of increased phenotypic variation (Burga et al. 2011; Bauer et al. 2015). For example, *BEH4*, the earliest diverged member of the *BZR/BEH* family of transcription factors, governs phenotypic robustness of hypocotyl length by integrating regulatory cross-talk among the six gene family members (Lachowiec et al. 2018). Thus, even among these closely related, partially redundant paralogs, increased trait variation arises when the activity of *BEH4* is lost. The loss of properly integrated regulatory cross-talk as a cause of increased phenotypic variation is consistent with our findings that upregulation of *LTP1* in the dark is associated with the *ltp2* phenotypes.

Subtle changes in gene expression that percolate through gene regulatory networks and amplify each other to affect expression of certain core genes are thought to underlie complex diseases and complex traits in humans (the omnigenic model, (Boyle et al. 2017; Liu et al. 2019)). The genetic variants found to be associated with complex diseases and traits in genome-wide association studies (GWAS) typically reside in regulatory regions, likely resulting in hypomorphs. The trait heritability explained by GWAS variants tends to be small, and these variants have little power to predict the disease risk of individuals (Eichler et al. 2010; Gibson 2012; Khera et al. 2018; Manolio et al. 2009). The low power to predict phenotype from genotype is consistent with high non-genetic trait variation (Queitsch et al. 2012). We speculate that this non-genetic variation arises because regulatory variants cause small expression changes that are integrated differently among individuals. In turn, these differences in integrating expression changes will sensitize certain individuals but not others to environmental factors, resulting in different phenotypes. At least for *LTP2*, this interpretation holds: the

upregulation of *LTP1* is not sufficient for the observed phenotypes as all *ltp2* seedlings exhibit it. Likewise, all *ltp2* seedlings experience exposure to sucrose; however, not all seedlings have short hypocotyls and show loss of cuticle integrity. The loss of barrier (*i.e*. cuticle) function in this plant example likely holds lessons for studies of human traits and diseases and points to genotype-by-environment effects as a major contributor to non-genetic variation.

Our study highlights that even highly inbred, *de facto* homozygous genetic backgrounds maintain a physiologically relevant reservoir of phenotypic variation, which can be exposed by stress. While stress often increases phenotypic variation in isogenic and inbred populations (Thattai and van Oudenaarden 2004; Braendle and Félix 2008; Tokatlidis et al. 2010; Holland et al. 2014; de Groot et al. 2022; Mitosch et al. 2017; Uyttewaal et al. 2012; Newman et al. 2006; Sandner et al. 2021), phenotypic robustness (*i.e*., low non-genetic variation) is associated with stress tolerance and vigor in crops and lifestock (Tollenaar and Lee 2002; Blasco et al. 2017; Elgersma et al. 2018). A common strategy to achieve phenotypic robustness coupled with high performance in agricultural settings has been the use of F1 hybrids, which are often more uniform in phenotype than their inbred parental lines (Lewis 1953; Phelan and Austad 1994; Smith et al. 1955). A better understanding of the mechanistic underpinnings of non-genetic phenotypic variation might lead to the development of crops and livestock that combine uniformity of phenotype with broad stress tolerance. This better understanding of non-genetic phenotypic variation will also facilitate efforts to unravel the complexity of non-Mendelian human traits and diseases.

MATERIALS AND METHODS

Plant Material *Arabidopsis thaliana*, all lines are in the Col-0 background. *ltp2-1* is SALK_026257 (ABRC), previously described (Jacq et al. 2017). *ltp2-1* plants homozygous for the T-DNA insertion (Chr2:16,128,007 SALK project) were confirmed by PCR analysis with primer pairs CA340 (Chr2:16,128,062) + CA103 (Chr2:16,128,340) and CA249 (Chr2:16,127,7702) + CA103 (primer sequences in Table S7). *ltp2-2* is line DT7-3 (Marjorie Matzke lab) previously described (Kanno et al. 2004); contains a transgene insertion located upstream of *LTP2*, mapped in Kanno et al., 2004. Approximate location is Chr2:16,128,261, determined by sequencing the PCR fragment CA340+CA103. *ltp2-2* plants were confirmed homozygous for the transgene insertion by PCR genotyping with the same primers as *ltp2-1*. The *ltp1ltp2* double knock-down line was generated by Agrobacterium-mediated (GV3101) co-transformation of Col-0 plants with the helper plasmid pSOUP (CD3-1124, ABRC) and the plasmid CSHL_0103F2 (ABRC), containing an artificial microRNA against both *LTP2* and *LTP1.* T0 seeds were selected on 15mg/ml phosphinotricin (PPT/BASTA); PPT-resistant T1 plants were then propagated on 25mg/ml PPT; only generations T3 and above, homozygous for the transgene, were used in hypocotyl assays.

Hypocotyl Assays *(1) Hypocotyl and root length:* Unless otherwise stated, all seed batches were single-seed descent. Seeds were sterilized, resuspended in 0.1% (w/v) Bacto agar (BD, Diagnostics) and spotted in a well-spaced fashion onto square plates containing 1x MS media

(Murashige & Skoog Basal Salt Mixture) pH 5.8, with 0.5g/l MES (Sigma-Aldrich), 0.3% Phytagel (Sigma-Aldrich) and 1% sucrose (w/v). Plates were double-sealed with Micropore surgical tape (3M) and stratified in the dark for 4 days at 4C. After stratification, plates were exposed to 3 hours of light, then placed in vertical racks, wrapped in aluminum foil and kept at 22C in a Conviron chamber (50% RH; 16h light/8h dark; ~ 100 µmol m2 s) for 7 days. For certain experiments, the age and media composition varied as indicated elsewhere. Genotype placement was randomized across racks, and each genotype was distributed over multiple plates per experiment. At 7d after stratification, plates were opened and imaged on a fixed stand. ImageJ was used to trace and measure hypocotyl and root length for every seedling. The hypocotyl was scored from the collet (hypocotyl/root transition zone) till the shoot apical meristem. Root length was used to infer late germination; outlier hypocotyls with < 5mm (at 7 days) were removed from the analysis. Despite our best efforts, hypocotyl elongation proved highly sensitive to random environmental effects, and differences of a few millimeters in mean were not uncommon between replicates, even when controlling for seed batch (see Figure S2A)

(2) Hypocotyl negative gravitropism: The angle between the shoot apical meristem and an imaginary vertical line, drawn starting at the base of the hypocotyl, was used to quantify the negative gravitropic response in dark-grown hypocotyls at 7d post-stratification. Data was expressed as deviations off vertical (in degrees), with vertical representing perfect negative gravitropism. Measurements were done on ImageJ, as described for hypocotyl length.

(3) Hypocotyl e*pidermal imaging*: The epidermal surface of dark-grown hypocotyls was imaged at 7d post-stratification. Whole seedlings were placed directly on a glass slide and the hypocotyl imaged using a Zeiss Axioplan microscope at 50x magnification.

(4)Toluidine Blue Assay Protocol based on Tanaka et al., 2003 but with a lower concentration of dye to avoid saturation in *ltp2*. Whole dark-grown seedlings were immersed in an aqueous solution of 0.02% (w/v) toluidine blue (Sigma) for 2mins with gentle shaking, then washed 3x with distilled water and left in water until imaging. ImageJ was used to determine hypocotyl length and the fraction of the total length stained with toluidine blue.

<u>Seed Size</u> Matched datasets of seed size and hypocotyl length were obtained by imaging the same plate twice: (1) after stratification, when seeds were fully imbibed, and (2) after 7days of growth in the dark. The position of the seed and the hypocotyl are the same in both pictures. Between 10-20 seeds were spotted per plate and several plates were employed per genotype. For imaging seeds, pictures were taken under a stereomicroscope, at 5x magnification. Seed area was measured in ImageJ using > 8-bit > Threshold (auto) > Analyze Particles, with settings: area, 5000-infinity; circularity >= 0.7.

<u>qRT-PCR</u> Seedling samples were either single individuals or pools of about 30 individuals. Unless otherwise stated, only the shoot was harvested (includes hypocotyl, cotyledons and shoot apical meristem). For roots, rosette leaves and flowers, all samples were pools; roots were excised from 7d old seedlings; rosette leaves and flowers from mature plants. RNA was extracted from LN2 frozen material using TRIZOL (Invitrogen) and DNase I treated. cDNA was synthesized from 250-500mg of total RNA with the RevertAid First Strand cDNA Synthesis kit

(Thermo Scientific). qRT-PCR was performed with LightCycler 480 SYBR Green I Master Mix (Roche). Relative gene expression was calculated as 2^-(Ct target - Ct reference), with either *AP2M*/AT5G46630, *UBC21*/AT5G25760 or *PP2A*/AT1G13320 as reference genes. Primers are listed in Table S7.

RNA-seq data

(1) Setup and sequencing: For each replicate of Col-0 and *ltp2-1*, seven hypocotyl assays were set up in parallel, each containing 64-70 seedlings. At day 7 after stratification, hypocotyl length was scored for each of the seven assays and from each, only the shoots of the 10 most extreme seedlings at either tail of the distribution (bottom and top 15th percentile) were collected as "short" and "long" samples, respectively. Each sample contained a total of 70 shoots, and corresponds to one replicate. The process was repeated to obtain a second biological replicate, in a total of eight samples (Col-L1, Col-L2, Col-S1, Col-S2, *ltp2*-L1, *ltp2*-L2, *ltp2*-S1, *ltp2*-S2). RNA was extracted from all samples in parallel using the SV Promega Total RNA System followed by NaCl/EtOH precipitation. Generation of RNA-seq libraries, multiplexing and sequencing was outsourced to GENEWIZ (GENEWIZ Inc., NJ). Each library was sequenced on four lanes and two flowcells of an Illumina HiSeq2500 in a 1x50bp SE format.

(2) Pseudoalignment of reads and estimation of transcript abundance was done using Kallisto (Bray et al. 2016).. The kallisto index was built with Arabidopsis thaliana TAIR10 cDNA models ftp://ftp.ensemblgenomes.org/pub/plants/release-50/fasta/arabidopsis_thaliana/cdna/Arabidopsis_thaliana.TAIR10.cdna.all.fa.gz. Transcript abundances were quantified with parameters –single -l 200 -s 20. Kallisto abundance files were parsed into R (v. 3.6.1) using tximport(). The tx2gene file and the TxDb object used TAIR10 annotations ftp://ftp.arabidopsis.org/home/tair/Genes/TAIR10_genome_release/TAIR10_gff3/TAIR10_GFF3_genes_transposons.gff.
The output was a matrix of estimated counts with 26923 rows (genes) and 8 columns (samples).

(3) Differentially Expressed Genes (DEGs) After non-specific filtering to remove all non-expressed genes (zero counts across all samples; 2,917 genes), and all genes which did not have at least 1 count in all samples (4,023), a filtered matrix of 19,983 genes x 8 samples was converted to integers and used as input for DESeq2 (Love et al. 2014), with parameters: condition = genotype x hypocotyl length, with 2 biological replicates per condition. Only genes with a log2FC >=1 & adjusted p-value <= 0.01 were called as DEGs. As high fold-changes are more frequent in genes with low baseline expression, we specifically chose a less stringent fold-change cut-off to avoid discarding genes with very high expression like *LTP2.* DEGs were obtained for four different pairwise comparisons: (1) Col-L *vs* Col-S, (2) Col-L *vs* *ltp2*-L, (3) Col-S *vs* ltp2-S and (4) *ltp2*-L *vs* *ltp2*-S (Tables S1-S4).

(4) Principal Component Analysis (PCA) prcomp() was applied to a transposed standardized matrix of log10(counts) with 19,983 rows x 8 columns.

(5) Gene Ontology (GO) enrichments were obtained with gProfiler (Raudvere et al. 2019) https://biit.cs.ut.ee/gprofiler/gost, with the input to DESeq2 (a list of 19,983 genes) as

background. Significant GO terms were shortlisted if fold-enrichment >= 2 & Bonferroni corrected p-value < 0.05. Query genesets were (1) the list of 584 DEGs between *ltp2*-L and *ltp2*-S and (2) the list of 1164 DEGs unique to the comparison Col-S and *ltp2*-S.

(6) Cuticle genes From the dataset in Li-Beisson et al.,(2013) we selected only genes with annotated roles in cutin or wax biosynthesis and/or deposition (groups Cuticle Synthesis & Transport 1, Fatty Acid Elongation & Wax Biosynthesis and Fatty Acid Synthesis). The curated list contained 224 genes (Table S6), of which 160 were present in our RNA-seq dataset (Table S6), and 21 were differentially expressed between Col-0 and *ltp2* (union set between Col-L vs *ltp2*-L and Col-S vs *ltp2*-S, 1717 DEGs); the hypergeometric test indicates this is a modest over-representation (p= 0.019).

Protein sequence tree of PR-14/LTP Type I proteins Protein sequences for PR-14/Type I LTP proteins (Arondel12 et al. 2000) were retrieved from NCBI: NP_181388.1 LTP1, NP_181387.1 LTP2, NP_568905.1 LTP3, NP_568904.1 LTP4, NP_190728.1 LTP5, NP_187489.1 LTP6, NP_973466.1 LTP7, NP_179428.1 LTP8, NP_179135.2 LTP9, NP_195807.1 LTP10, NP_680758.3 LTP11, NP_190727.1 LTP12, NP_001078707.1 LTP13, NP_001078780.1 LTP14, NP_192593.3 LTP15. Multiple sequence alignment was done with ClustalW in the msa package (Bodenhofer et al. 2015) and the neighbor-joining tree with the ape package (Paradis et al. 2004).

LTP1 and *LTP2* global expression pattern We used the Digital Expression Explorer 2 repository (Ziemann et al. 2019) https://dee2.io/ to retrieve uniformly processed RNA-seq data from Arabidopsis thaliana. We curated a dataset of 56 samples, spanning several organs, contexts and developmental stages (Table S8), and kept only genes with at least 3 counts in one sample out of the 56 (26,372 genes x 56 samples).

DATA ACCESS

RNA-seq data is available at GEO (https://www.ncbi.nlm.nih.gov/geo/) BioProject ID PRJNA856271.

ACKNOWLEDGEMENTS

This work was supported by the National Science Foundation (NSF MCB-1242744, RESEARCH-PGR grant 1748843, PlantSynBio 2240888 to C.Q.) and the National Institute of Health (NIH NHGRI 5RM1HG010461, NIH NIGMS R35GM139532 to C.Q.)

REFERENCES

Abley K, Formosa-Jordan P, Tavares H, Chan EYT, Afsharinafar M, Leyser O, Locke JCW. 2021. An ABA-GA bistable switch can account for natural variation in the variability of Arabidopsis seed germination time. *Elife* **10**: e59485.

Ansel J, Bottin H, Rodriguez-Beltran C, Damon C, Nagarajan M, Fehrmann S, François J, Yvert G. 2008. Cell-to-cell stochastic variation in gene expression is a complex genetic trait. *PLoS Genet* **4**: e1000049.

Arondel12 V V, Vergnolle2 C, Cantrel C, Kader J. 2000. Lipid transfer proteins are encoded by a small multigene family in Arabidopsis thaliana. *Plant Sci* **157**: 1–12.

Ayroles JF, Buchanan SM, O'Leary C, Skutt-Kakaria K, Grenier JK, Clark AG, Hartl DL, de Bivort BL. 2015. Behavioral idiosyncrasy reveals genetic control of phenotypic variability. *Proc Natl Acad Sci U S A* **112**: 6706–6711.

Bauer CR, Li S, Siegal ML. 2015. Essential gene disruptions reveal complex relationships between phenotypic robustness, pleiotropy, and fitness. *Mol Syst Biol* **11**: 773.

Bessire M, Chassot C, Jacquat A-C, Humphry M, Borel S, Petétot JM-C, Métraux J-P, Nawrath C. 2007. A permeable cuticle in Arabidopsis leads to a strong resistance to Botrytis cinerea. *EMBO J* **26**: 2158–2168.

Blake WJ, KAErn M, Cantor CR, Collins JJ. 2003. Noise in eukaryotic gene expression. *Nature* **422**: 633–637.

Blasco A, Martínez-Álvaro M, García M-L, Ibáñez-Escriche N, Argente M-J. 2017. Selection for environmental variance of litter size in rabbits. *Genet Sel Evol* **49**: 48.

Bodenhofer U, Bonatesta E, Horejš-Kainrath C, Hochreiter S. 2015. msa: an R package for multiple sequence alignment. *Bioinformatics* **31**: 3997–3999.

Borevitz JO, Maloof JN, Lutes J, Dabi T, Redfern JL, Trainer GT, Werner JD, Asami T, Berry CC, Weigel D, et al. 2002. Quantitative trait loci controlling light and hormone response in two accessions of Arabidopsis thaliana. *Genetics* **160**: 683–696.

Boyle EA, Li YI, Pritchard JK. 2017. An expanded view of complex traits: From polygenic to omnigenic. *Cell* **169**: 1177–1186.

Braendle C, Félix M-A. 2008. Plasticity and errors of a robust developmental system in different environments. *Dev Cell* **15**: 714–724.

Bray NL, Pimentel H, Melsted P, Pachter L. 2016. Near-optimal probabilistic RNA-seq quantification. *Nat Biotechnol* **34**: 525–527.

Buhot N, Douliez JP, Jacquemard A, Marion D, Tran V, Maume BF, Milat ML, Ponchet M, Mikès V, Kader JC, et al. 2001. A lipid transfer protein binds to a receptor involved in the control of plant defence responses. *FEBS Lett* **509**: 27–30.

Burga A, Casanueva MO, Lehner B. 2011. Predicting mutation outcome from early stochastic variation in genetic interaction partners. *Nature* **480**: 250–253.

Cameron KD, Teece MA, Smart LB. 2006. Increased accumulation of cuticular wax and expression of lipid transfer protein in response to periodic drying events in leaves of tree tobacco. *Plant Physiol* **140**: 176–183.

Casanueva MO, Burga A, Lehner B. 2012. Fitness trade-offs and environmentally induced mutation buffering in isogenic C. elegans. *Science* **335**: 82–85.

Chae K, Gonong BJ, Kim S-C, Kieslich CA, Morikis D, Balasubramanian S, Lord EM. 2010. A multifaceted study of stigma/style cysteine-rich adhesin (SCA)-like Arabidopsis lipid transfer proteins (LTPs) suggests diversified roles for these LTPs in plant growth and

reproduction. *J Exp Bot* **61**: 4277–4290.

Chae K, Kieslich CA, Morikis D, Kim S-C, Lord EM. 2009. A gain-of-function mutation of Arabidopsis lipid transfer protein 5 disturbs pollen tube tip growth and fertilization. *Plant Cell* **21**: 3902–3914.

Chassot C, Nawrath C, Métraux J-P. 2007. Cuticular defects lead to full immunity to a major plant pathogen. *Plant J* **49**: 972–980.

Chen X, Goodwin SM, Boroff VL, Liu X, Jenks MA. 2003. Cloning and characterization of the WAX2 gene of Arabidopsis involved in cuticle membrane and wax production. *Plant Cell* **15**: 1170–1185.

Dandage R, Landry CR. 2019. Paralog dependency indirectly affects the robustness of human cells. *Mol Syst Biol* **15**: e8871.

de Groot DH, Tjalma AJ, Bruggeman FJ, van Nimwegen E. 2022. Coupling phenotype stability to growth rate overcomes limitations of bet-hedging strategies. *bioRxiv* 2022.04.12.488059. https://www.biorxiv.org/content/10.1101/2022.04.12.488059v1.full (Accessed July 29, 2022).

Dean EJ, Davis JC, Davis RW, Petrov DA. 2008. Pervasive and persistent redundancy among duplicated genes in yeast. *PLoS Genet* **4**: e1000113.

Debono A, Yeats TH, Rose JKC, Bird D, Jetter R, Kunst L, Samuels L. 2009. Arabidopsis LTPG is a glycosylphosphatidylinositol-anchored lipid transfer protein required for export of lipids to the plant surface. *Plant Cell* **21**: 1230–1238.

Deeken R, Saupe S, Klinkenberg J, Riedel M, Leide J, Hedrich R, Mueller TD. 2016. The Nonspecific Lipid Transfer Protein AtLtpI-4 Is Involved in Suberin Formation of Arabidopsis thaliana Crown Galls. *Plant Physiol* **172**: 1911–1927.

DeLuna A, Springer M, Kirschner MW, Kishony R. 2010. Need-based up-regulation of protein levels in response to deletion of their duplicate genes. *PLoS Biol* **8**: e1000347.

DeLuna A, Vetsigian K, Shoresh N, Hegreness M, Colón-González M, Chao S, Kishony R. 2008. Exposing the fitness contribution of duplicated genes. *Nat Genet* **40**: 676–681.

Delvigne F, Zune Q, Lara AR, Al-Soud W, Sørensen SJ. 2014. Metabolic variability in bioprocessing: implications of microbial phenotypic heterogeneity. *Trends Biotechnol* **32**: 608–616.

Derbyshire P, Findlay K, McCann MC, Roberts K. 2007. Cell elongation in Arabidopsis hypocotyls involves dynamic changes in cell wall thickness. *J Exp Bot* **58**: 2079–2089.

Diss G, Ascencio D, DeLuna A, Landry CR. 2014. Molecular mechanisms of paralogous compensation and the robustness of cellular networks. *J Exp Zool B Mol Dev Evol* **322**: 488–499.

Diss G, Gagnon-Arsenault I, Dion-Coté A-M, Vignaud H, Ascencio DI, Berger CM, Landry CR. 2017. Gene duplication can impart fragility, not robustness, in the yeast protein interaction network. *Science* **355**: 630–634.

Eagle H, Levine EM. 1967. Growth regulatory effects of cellular interaction. *Nature* **213**: 1102–1106.

Eichler EE, Flint J, Gibson G, Kong A, Leal SM, Moore JH, Nadeau JH. 2010. Missing heritability and strategies for finding the underlying causes of complex disease. *Nat Rev Genet* **11**: 446–450.

Eldar A, Chary VK, Xenopoulos P, Fontes ME, Losón OC, Dworkin J, Piggot PJ, Elowitz MB. 2009. Partial penetrance facilitates developmental evolution in bacteria. *Nature* **460**: 510–514.

Elgersma GG, de Jong G, van der Linde R, Mulder HA. 2018. Fluctuations in milk yield are heritable and can be used as a resilience indicator to breed healthy cows. *J Dairy Sci* **101**: 1240–1250.

Elowitz MB, Levine AJ, Siggia ED, Swain PS. 2002. Stochastic gene expression in a single cell. *Science* **297**: 1183–1186.

Emert BL, Cote CJ, Torre EA, Dardani IP, Jiang CL, Jain N, Shaffer SM, Raj A. 2021. Variability within rare cell states enables multiple paths toward drug resistance. *Nat Biotechnol* **39**: 865–876.

Feinerman O, Veiga J, Dorfman JR, Germain RN, Altan-Bonnet G. 2008. Variability and robustness in T cell activation from regulated heterogeneity in protein levels. *Science* **321**: 1081–1084.

Finch-Savage WE, Bassel GW. 2016. Seed vigour and crop establishment: extending performance beyond adaptation. *J Exp Bot* **67**: 567–591.

Finkina EI, Melnikova DN, Bogdanov IV, Ovchinnikova TV. 2016. Lipid Transfer Proteins As Components of the Plant Innate Immune System: Structure, Functions, and Applications. *Acta Naturae* **8**: 47–61.

Gao S, Guo W, Feng W, Liu L, Song X, Chen J, Hou W, Zhu H, Tang S, Hu J. 2016. LTP3 contributes to disease susceptibility in Arabidopsis by enhancing abscisic acid (ABA) biosynthesis. *Mol Plant Pathol* **17**: 412–426.

Geldner N. 2013. The endodermis. *Annu Rev Plant Biol* **64**: 531–558.

Gendreau E, Traas J, Desnos T, Grandjean O, Caboche M, Höfte H. 1997. Cellular basis of hypocotyl growth in Arabidopsis thaliana. *Plant Physiol* **114**: 295–305.

Gibson G. 2012. Rare and common variants: twenty arguments. *Nat Rev Genet* **13**: 135–145.

Gimelbrant A, Hutchinson JN, Thompson BR, Chess A. 2007. Widespread monoallelic expression on human autosomes. *Science* **318**: 1136–1140.

Gu Z, Steinmetz LM, Gu X, Scharfe C, Davis RW, Li W-H. 2003. Role of duplicate genes in genetic robustness against null mutations. *Nature* **421**: 63–66.

Hall MC, Dworkin I, Ungerer MC, Purugganan M. 2007. Genetics of microenvironmental canalization in Arabidopsis thaliana. *Proc Natl Acad Sci U S A* **104**: 13717–13722.

Hartwell LH, Culotti J, Pringle JR, Reid BJ. 1974. Genetic control of the cell division cycle in yeast. *Science* **183**: 46–51.

Hill WG, Mulder HA, Zhang X-S. 2007. The quantitative genetics of phenotypic variation in animals. *Acta Agric Scand A Anim Sci* **57**: 175–182.

Holland SL, Reader T, Dyer PS, Avery SV. 2014. Phenotypic heterogeneity is a selected trait in natural yeast populations subject to environmental stress. *Environ Microbiol* **16**: 1729–1740.

Hong L, Dumond M, Tsugawa S, Sapala A, Routier-Kierzkowska A-L, Zhou Y, Chen C, Kiss A, Zhu M, Hamant O, et al. 2016. Variable Cell Growth Yields Reproducible OrganDevelopment through Spatiotemporal Averaging. *Dev Cell* **38**: 15–32.

Ihmels J, Collins SR, Schuldiner M, Krogan NJ, Weissman JS. 2007. Backup without redundancy: genetic interactions reveal the cost of duplicate gene loss. *Mol Syst Biol* **3**: 86.

Illouz-Eliaz N, Ramon U, Shohat H, Blum S, Livne S, Mendelson D, Weiss D. 2019. Multiple Gibberellin Receptors Contribute to Phenotypic Stability under Changing Environments. *Plant Cell* **31**: 1506–1519.

Irshad M, Canut H, Borderies G, Pont-Lezica R, Jamet E. 2008. A new picture of cell wall protein dynamics in elongating cells of Arabidopsis thaliana: confirmed actors and newcomers. *BMC Plant Biol* **8**: 94.

Jacq A, Pernot C, Martinez Y, Domergue F, Payré B, Jamet E, Burlat V, Pacquit VB. 2017. The Arabidopsis Lipid Transfer Protein 2 (AtLTP2) Is Involved in Cuticle-Cell Wall Interface Integrity and in Etiolated Hypocotyl Permeability. *Front Plant Sci* **8**: 263.

Jimenez-Gomez JM, Corwin JA, Joseph B, Maloof JN, Kliebenstein DJ. 2011. Genomic analysis of QTLs and genes altering natural variation in stochastic noise. *PLoS Genet* **7**: e1002295.

Joseph B, Corwin JA, Kliebenstein DJ. 2015. Genetic variation in the nuclear and organellar genomes modulates stochastic variation in the metabolome, growth, and defense. *PLoS Genet* **11**: e1004779.

Kader J-C. 1996. LIPID-TRANSFER PROTEINS IN PLANTS. *Annu Rev Plant Physiol Plant Mol Biol* **47**: 627–654.

Kafri R, Bar-Even A, Pilpel Y. 2005. Transcription control reprogramming in genetic backup circuits. *Nat Genet* **37**: 295–299.

Kanno T, Mette MF, Kreil DP, Aufsatz W, Matzke M, Matzke AJM. 2004. Involvement of putative SNF2 chromatin remodeling protein DRD1 in RNA-directed DNA methylation. *Curr Biol* **14**: 801–805.

Karahara I. 2012. The pea stem: a unique experimental system to study the development of the Casparian strip. *Plant Signal Behav* **7**: 1182–1184.

Katsanos D, Koneru SL, Mestek Boukhibar L, Gritti N, Ghose R, Appleford PJ, Doitsidou M, Woollard A, van Zon JS, Poole RJ, et al. 2017. Stochastic loss and gain of symmetric

divisions in the C. elegans epidermis perturbs robustness of stem cell number. *PLoS Biol* **15**: e2002429.

Khera AV, Chaffin M, Aragam KG, Haas ME, Roselli C, Choi SH, Natarajan P, Lander ES, Lubitz SA, Ellinor PT, et al. 2018. Genome-wide polygenic scores for common diseases identify individuals with risk equivalent to monogenic mutations. *Nat Genet* **50**: 1219–1224.

Kircher S, Schopfer P. 2012. Photosynthetic sucrose acts as cotyledon-derived long-distance signal to control root growth during early seedling development in Arabidopsis. *Proc Natl Acad Sci U S A* **109**: 11217–11221.

Kurdyukov S, Faust A, Nawrath C, Bär S, Voisin D, Efremova N, Franke R, Schreiber L, Saedler H, Métraux J-P, et al. 2006. The epidermis-specific extracellular BODYGUARD controls cuticle development and morphogenesis in Arabidopsis. *Plant Cell* **18**: 321–339.

Lachowiec J, Mason GA, Schultz K, Queitsch C. 2018. Redundancy, Feedback, and Robustness in the Arabidopsis thaliana BZR/BEH Gene Family. *Front Genet* **9**: 523.

Lachowiec J, Queitsch C, Kliebenstein DJ. 2016. Molecular mechanisms governing differential robustness of development and environmental responses in plants. *Ann Bot* **117**: 795–809.

Lemus T, Mason GA, Bubb KL, Alexandre CM, Queitsch C, Cuperus JT. 2023. AGO1 and HSP90 buffer different genetic variants in Arabidopsis thaliana. *Genetics* **223**. http://dx.doi.org/10.1093/genetics/iyac163.

Lewis D. 1953. A relationship between dominance, phenotypic stability and variability, and a theory of alternative genetic pathways. *Nature* **172**: 1136–1137.

L'Haridon F, Besson-Bard A, Binda M, Serrano M, Abou-Mansour E, Balet F, Schoonbeek H-J, Hess S, Mir R, Léon J, et al. 2011. A permeable cuticle is associated with the release of reactive oxygen species and induction of innate immunity. *PLoS Pathog* **7**: e1002148.

Li-Beisson Y, Shorrosh B, Beisson F, Andersson MX, Arondel V, Bates PD, Baud S, Bird D, Debono A, Durrett TP, et al. 2013. Acyl-lipid metabolism. *Arabidopsis Book* **11**: e0161.

Liu X, Li YI, Pritchard JK. 2019. Trans effects on gene expression can drive omnigenic inheritance. *Cell* **177**: 1022-1034.e6.

Lolle SJ, Cheung AY, Sussex IM. 1992. Fiddlehead: an Arabidopsis mutant constitutively expressing an organ fusion program that involves interactions between epidermal cells. *Dev Biol* **152**: 383–392.

Lomvardas S, Barnea G, Pisapia DJ, Mendelsohn M, Kirkland J, Axel R. 2006. Interchromosomal interactions and olfactory receptor choice. *Cell* **126**: 403–413.

Love MI, Huber W, Anders S. 2014. Moderated estimation of fold change and dispersion for RNA-seq data with DESeq2. *Genome Biol* **15**: 550.

Maldonado AM, Doerner P, Dixon RA, Lamb CJ, Cameron RK. 2002. A putative lipid transfer protein involved in systemic resistance signalling in Arabidopsis. *Nature* **419**: 399–403.

Maloof JN, Borevitz JO, Dabi T, Lutes J, Nehring RB, Redfern JL, Trainer GT, Wilson JM, Asami T, Berry CC, et al. 2001. Natural variation in light sensitivity of Arabidopsis. *Nat Genet* **29**: 441–446.

Manolio TA, Collins FS, Cox NJ, Goldstein DB, Hindorff LA, Hunter DJ, McCarthy MI, Ramos EM, Cardon LR, Chakravarti A, et al. 2009. Finding the missing heritability of complex diseases. *Nature* **461**: 747–753.

Márquez-Jurado S, Díaz-Colunga J, das Neves RP, Martinez-Lorente A, Almazán F, Guantes R, Iborra FJ. 2018. Mitochondrial levels determine variability in cell death by modulating apoptotic gene expression. *Nat Commun* **9**: 389.

Mason GA, Lemus T, Queitsch C. 2016. The mechanistic underpinnings of an ago1-mediated, environmentally dependent, and stochastic phenotype. *Plant Physiol* **170**: 2420–2431.

Miedes E, Suslov D, Vandenbussche F, Kenobi K, Ivakov A, Van Der Straeten D, Lorences EP, Mellerowicz EJ, Verbelen J-P, Vissenberg K. 2013. Xyloglucan endotransglucosylase/hydrolase (XTH) overexpression affects growth and cell wall mechanics in etiolated Arabidopsis hypocotyls. *J Exp Bot* **64**: 2481–2497.

Mitosch K, Rieckh G, Bollenbach T. 2017. Noisy Response to Antibiotic Stress Predicts Subsequent Single-Cell Survival in an Acidic Environment. *Cell Syst* **4**: 393-403.e5.

Molina A, Segura A, García-Olmedo F. 1993. Lipid transfer proteins (nsLTPs) from barley and maize leaves are potent inhibitors of bacterial and fungal plant pathogens. *FEBS Lett* **316**: 119–122.

Morgante F, Sørensen P, Sorensen DA, Maltecca C, Mackay TFC. 2015. Genetic Architecture of Micro-Environmental Plasticity in Drosophila melanogaster. *Sci Rep* **5**: 9785.

Narukawa H, Yokoyama R, Nishitani K. 2016. Possible pathways linking ploidy level to cell elongation and cuticular function in hypocotyls of dark-grown Arabidopsis seedlings. *Plant Signal Behav* **11**: e1118597.

Newman JRS, Ghaemmaghami S, Ihmels J, Breslow DK, Noble M, DeRisi JL, Weissman JS. 2006. Single-cell proteomic analysis of S. cerevisiae reveals the architecture of biological noise. *Nature* **441**: 840–846.

Nieuwland J, Feron R, Huisman BAH, Fasolino A, Hilbers CW, Derksen J, Mariani C. 2005. Lipid transfer proteins enhance cell wall extension in tobacco. *Plant Cell* **17**: 2009–2019.

Paradis E, Claude J, Strimmer K. 2004. APE: Analyses of Phylogenetics and Evolution in R language. *Bioinformatics* **20**: 289–290.

Park J-E, Kim Y-S, Yoon H-K, Park C-M. 2007. Functional characterization of a small auxin-up RNA gene in apical hook development in Arabidopsis. *Plant Sci* **172**: 150–157.

Perez MF, Francesconi M, Hidalgo-Carcedo C, Lehner B. 2017. Maternal age generates phenotypic variation in Caenorhabditis elegans. *Nature* **552**: 106–109.

Phelan JP, Austad SN. 1994. Selecting animal models of human aging: inbred strains often exhibit less biological uniformity than F1 hybrids. *J Gerontol* **49**: B1-11.

Potocka I, Baldwin TC, Kurczynska EU. 2012. Distribution of lipid transfer protein 1 (LTP1) epitopes associated with morphogenic events during somatic embryogenesis of Arabidopsis thaliana. *Plant Cell Rep* **31**: 2031–2045.

Queitsch C, Carlson KD, Girirajan S. 2012. Lessons from model organisms: phenotypic robustness and missing heritability in complex disease. *PLoS Genet* **8**: e1003041.

Queitsch C, Sangster TA, Lindquist S. 2002. Hsp90 as a capacitor of phenotypic variation. *Nature* **417**: 618–624.

Rai MI, Wang X, Thibault DM, Kim HJ, Bombyk MM, Binder BM, Shakeel SN, Eric Schaller G. 2015. The ARGOS gene family functions in a negative feedback loop to desensitize plants to ethylene. *BMC Plant Biol* **15**: 1–14.

Raj A, Rifkin SA, Andersen E, van Oudenaarden A. 2010. Variability in gene expression underlies incomplete penetrance. *Nature* **463**: 913–918.

Raser JM, O'Shea EK. 2004. Control of stochasticity in eukaryotic gene expression. *Science* **304**: 1811–1814.

Raudvere U, Kolberg L, Kuzmin I, Arak T, Adler P, Peterson H, Vilo J. 2019. g:Profiler: a web server for functional enrichment analysis and conversions of gene lists (2019 update). *Nucleic Acids Res* **47**: W191–W198.

Reed JW, Elumalai RP, Chory J. 1998. Suppressors of an Arabidopsis thaliana phyB mutation identify genes that control light signaling and hypocotyl elongation. *Genetics* **148**: 1295–1310.

Ros M, Sorensen D, Waagepetersen R, Dupont-Nivet M, SanCristobal M, Bonnet J-C, Mallard J. 2004. Evidence for genetic control of adult weight plasticity in the snail Helix aspersa. *Genetics* **168**: 2089–2097.

Sandner TM, Matthies D, Waller DM. 2021. Stresses affect inbreeding depression in complex ways: disentangling stress-specific genetic effects from effects of initial size in plants. *Heredity* **127**: 347–356.

Sangster TA, Salathia N, Undurraga S, Milo R, Schellenberg K, Lindquist S, Queitsch C. 2008. HSP90 affects the expression of genetic variation and developmental stability in quantitative traits. *Proc Natl Acad Sci U S A* **105**: 2963–2968.

Sawa S, Ohgishi M, Goda H, Higuchi K, Shimada Y, Yoshida S, Koshiba T. 2002. The HAT2 gene, a member of the HD-Zip gene family, isolated as an auxin inducible gene by DNA microarray screening, affects auxin response in Arabidopsis. *Plant J* **32**: 1011–1022.

Schnurr J, Shockey J, Browse J. 2004. The acyl-CoA synthetase encoded by LACS2 is essential for normal cuticle development in Arabidopsis. *Plant Cell* **16**: 629–642.

Serrano M, Coluccia F, Torres M, L'Haridon F, Métraux J-P. 2014. The cuticle and plant defense to pathogens. *Front Plant Sci* **5**: 274.

Shaffer SM, Dunagin MC, Torborg SR, Torre EA, Emert B, Krepler C, Beqiri M, Sproesser K, Brafford PA, Xiao M, et al. 2017. Rare cell variability and drug-induced reprogramming as a mode of cancer drug resistance. *Nature* **546**: 431–435.

Sharma SV, Lee DY, Li B, Quinlan MP, Takahashi F, Maheswaran S, McDermott U, Azizian N, Zou L, Fischbach MA, et al. 2010. A chromatin-mediated reversible drug-tolerant state in cancer cell subpopulations. *Cell* **141**: 69–80.

Shen X, Pettersson M, Rönnegård L, Carlborg Ö. 2012. Inheritance beyond plain heritability: variance-controlling genes in Arabidopsis thaliana. *PLoS Genet* **8**: e1002839.

Sieber P, Schorderet M, Ryser U, Buchala A, Kolattukudy P, Métraux JP, Nawrath C. 2000. Transgenic Arabidopsis plants expressing a fungal cutinase show alterations in the structure and properties of the cuticle and postgenital organ fusions. *Plant Cell* **12**: 721–738.

Smith JM, Clarke JM, Hollingsworth MJ. 1955. The expression of hybrid vigour in Drosophila subobscura. *Proc R Soc Lond B Biol Sci* **144**: 159–171.

Smith MCA, Sumner ER, Avery SV. 2007. Glutathione and Gts1p drive beneficial variability in the cadmium resistances of individual yeast cells. *Mol Microbiol* **66**: 699–712.

Snijder B, Sacher R, Rämö P, Damm E-M, Liberali P, Pelkmans L. 2009. Population context determines cell-to-cell variability in endocytosis and virus infection. *Nature* **461**: 520–523.

Spartz AK, Lee SH, Wenger JP, Gonzalez N, Itoh H, Inzé D, Peer WA, Murphy AS, Overvoorde PJ, Gray WM. 2012. The SAUR19 subfamily of SMALL AUXIN UP RNA genes promote cell expansion. *Plant J* **70**: 978–990.

Takahashi K, Shimada T, Kondo M, Tamai A, Mori M, Nishimura M, Hara-Nishimura I. 2010. Ectopic expression of an esterase, which is a candidate for the unidentified plant cutinase, causes cuticular defects in Arabidopsis thaliana. *Plant Cell Physiol* **51**: 123–131.

Tanaka T, Tanaka H, Machida C, Watanabe M, Machida Y. 2004. A new method for rapid visualization of defects in leaf cuticle reveals five intrinsic patterns of surface defects in Arabidopsis. *Plant J* **37**: 139–146.

Thattai M, van Oudenaarden A. 2004. Stochastic gene expression in fluctuating environments. *Genetics* **167**: 523–530.

Tian Q, Uhlir NJ, Reed JW. 2002. Arabidopsis SHY2/IAA3 inhibits auxin-regulated gene expression. *Plant Cell* **14**: 301–319.

Tokatlidis IS, Haş V, Mylonas I, Haş I, Evgenidis G, Melidis V, Copandean A, Ninou E. 2010. Density effects on environmental variance and expected response to selection in maize (Zea mays L.). *Euphytica* **174**: 283–291.

Tollenaar M, Lee EA. 2002. Yield potential, yield stability and stress tolerance in maize. *Field Crops Res* **75**: 161–169.

Tran DT, Hertog MLATM, Tran TLH, Quyen NT, Van de Poel B, Mata CI, Nicolaï BM. 2017. Population Modeling Approach to Optimize Crop Harvest Strategy. The Case of Field Tomato. *Front Plant Sci* **8**: 608.

Uyttewaal M, Burian A, Alim K, Landrein B, Borowska-Wykręt D, Dedieu A, Peaucelle A,

Ludynia M, Traas J, Boudaoud A, et al. 2012. Mechanical stress acts via katanin to amplify differences in growth rate between adjacent cells in Arabidopsis. *Cell* **149**: 439–451.

van Heerden JH, Wortel MT, Bruggeman FJ, Heijnen JJ, Bollen YJM, Planqué R, Hulshof J, O'Toole TG, Wahl SA, Teusink B. 2014. Lost in transition: start-up of glycolysis yields subpopulations of nongrowing cells. *Science* **343**: 1245114.

Vandenbussche F, Verbelen J-P, Van Der Straeten D. 2005. Of light and length: regulation of hypocotyl growth in Arabidopsis. *Bioessays* **27**: 275–284.

Volfson D, Marciniak J, Blake WJ, Ostroff N, Tsimring LS, Hasty J. 2006. Origins of extrinsic variability in eukaryotic gene expression. *Nature* **439**: 861–864.

Waddington CH. 1942. CANALIZATION OF DEVELOPMENT AND THE INHERITANCE OF ACQUIRED CHARACTERS. *Nature* **150**: 563–565.

Wellesen K, Durst F, Pinot F, Benveniste I, Nettesheim K, Wisman E, Steiner-Lange S, Saedler H, Yephremov A. 2001. Functional analysis of the LACERATA gene of Arabidopsis provides evidence for different roles of fatty acid omega -hydroxylation in development. *Proc Natl Acad Sci U S A* **98**: 9694–9699.

Whitlock MC, Fowler K. 1999. The changes in genetic and environmental variance with inbreeding in Drosophila melanogaster. *Genetics* **152**: 345–353.

Wright S. 1920. The Relative Importance of Heredity and Environment in Determining the Piebald Pattern of Guinea-Pigs. *Proc Natl Acad Sci U S A* **6**: 320–332.

Xiao C, Somerville C, Anderson CT. 2014. POLYGALACTURONASE INVOLVED IN EXPANSION1 functions in cell elongation and flower development in Arabidopsis. *Plant Cell* **26**: 1018–1035.

Xiao Y, Bowen CH, Liu D, Zhang F. 2016. Exploiting nongenetic cell-to-cell variation for enhanced biosynthesis. *Nat Chem Biol* **12**: 339–344.

Yeats TH, Rose JKC. 2008. The biochemistry and biology of extracellular plant lipid-transfer proteins (LTPs). *Protein Sci* **17**: 191–198.

Zabinsky RA, Mason GA, Queitsch C, Jarosz DF. 2019. It's not magic – Hsp90 and its effects on genetic and epigenetic variation. *Semin Cell Dev Biol* **88**: 21–35.

Ziemann M, Kaspi A, El-Osta A. 2019. Digital expression explorer 2: a repository of uniformly processed RNA sequencing data. *Gigascience* **8**. http://dx.doi.org/10.1093/gigascience/giz022.

FIGURE LEGENDS

Figure 1. *LTP2* hypomorphs increase phenotypic variation in skotomorphogenesis traits. **A**. Approximate location of the T-DNA insertion (LB) relative to the *LTP2* gene in *ltp2-1* and *ltp2-2* lines. **B**. *LTP2* relative expression in the shoots of wild-type (Col-0), *ltp2-1* and *ltp2-2* seedlings

grown in the dark for 7 days (d) after stratification. In parenthesis is the % of Col-0 *LTP2* levels detected in the *ltp2* lines. **C**. Representative image of Col-0 (top), *ltp2-1* (middle) and *ltp2-2* (bottom) dark-grown seedlings at 7 days after stratification; the roots were trimmed. **D**. Density lines of the distributions of hypocotyl length scored at 7 days post-stratification in Col-0 and *ltp2*; each line represents the merged distribution of 5 biological replicates (*n*=78-210 each) per genotype. **E**. Coefficient of variation (sd/mean) in hypocotyl length, a measure of variation, for (1) 5 biological replicates (open circles) and (2) merged for all 5 replicates (filled circle, same data as in **D**). **F**. Hypocotyl negative gravitropism measured as the deviation from vertical (in degrees) of the hypocotyl apex in 7d dark-grown seedlings. The density distribution of measured angles for all genotypes is plotted. **G**. Comparison between the hypocotyl length of individual *ltp2* parents (5 long and 5 short) and the mean hypocotyl length of their offspring; all lengths measured at 7d post-stratification. **H**. Beanplots of hypocotyl (left side) and root (right side) length from the merged dataset used in **D** and **E**. **I**. Percentage of cotyledon phenotype as open (open circles) or closed (filled circles) for indicated number of wild-type (Col-0), *ltp2-1* and *ltp2-2* seedlings grown in the dark for 7 days after stratification. Two replicates are shown (n=79-208 replicates).

Figure 2. Sucrose-dependent loss of cuticle integrity in *ltp2* is associated with short hypocotyls. **A**. Density lines of the distribution of hypocotyl length for seedlings grown on plates containing MS medium, MS+1% glucose or MS+1% sucrose for 7 days post-stratification. Shown are the merged distributions of two biological replicates per condition/per genotype. **B**. Coefficient of variation in hypocotyl length for the distributions shown in **A**. **C**. Representative shoots of 7d dark-grown seedlings grown on plates containing MS medium, MS+1% glucose or MS+1% sucrose. Hypocotyl negative gravitropism is largely rescued in *ltp2* seedlings grown without sucrose. **D**. Boxplots comparing the hypocotyl/root ratio for every seedling in **A** across different growth media. **E**. Magnified images of the epidermal surface of Col-0 and *ltp2-1* hypocotyls at 7d post-stratification when grown with (left) or without (right) 1% sucrose. **F**. Comparing the effects of 1% sucrose on hypocotyl cuticle permeability: dark-grown seedlings of Col-0 and *ltp2-1* were stained with toluidine blue after growing for 5 days on MS+1% sucrose (left) or 7 days on MS alone (right). **G**. Relationship between hypocotyl length at 7 days after stratification and toluidine blue staining coverage expressed in % of hypocotyl length. Filled dots represent seedlings with the wild-type developmental pattern of hypocotyls > roots.

Figure 3. Hypocotyl length is associated with many transcriptional differences in *ltp2* but not Col-0 seedlings, mostly related to stress, defense and growth. **A**. Experimental setup for collecting RNA-seq samples. For Col-0 and *ltp2-1*, the first boxplot shows the distribution of hypocotyl length from one out of seven hypocotyl assays done per replicate; the second set of four boxplots (two replicates with short and two replicates with long hypocotyls) shows the actual distribution of hypocotyl lengths (n=70) from the selected individuals used to generate RNA-seq libraries. **B**. Biplot of Principal Component Analysis showing the first two PCs. The percentage of the total variance explained by PC1 and PC2 is indicated on the top right corner. **C**. Correlation between mean hypocotyl length for the eight RNA-seq samples and PC1 loadings; shown on the bottom left corner is the Spearman rho. **D**. Shortlisted GO enrichments (fold-enrichment >=2 and adjusted p-value < 0.05) for the set of 584 differentially expressed genes between *ltp2*-L and *ltp2*-S, split by down- and upregulated genes. Shown are the log10(fold-enrichment) and the number of DEGs per enriched term. **E-F** Row-scaled heatmap visualizations of a subset of DEGs

downregulated (**E**) or upregulated (**F**) in *ltp2*-S relative to *ltp2*-L. Pink dots indicate whether each gene was also a DEG on other pairwise-comparisons.

Figure 4. The *ltp2* phenotype depends on the expression ration of *LTP2* and its close paralog *LTP1* **A**. Row-scaled heatmap visualization of cuticle-related genes differentially expressed between Col-0 and *ltp2* samples. **B**. Detail of a tree depicting aminoacid sequence similarity among PR14/Type I LTP proteins (full tree in Figure S5A). **C**. Relative expression of *LTP1* and *LTP2* in the shoots of light or dark-grown (gray box) Col-0 and *ltp2* seedlings grown for 7 days after stratification. **D**. Comparison of the *LTP1/LTP2* ratio between Col-0, *ltp2-1* and an *ltp1ltp2* double mutant. **E-G** Hypocotyl length distribution (**E**), coefficient of variation of hypocotyl length (**F**) and (**G**) hypocotyl/root ratio for Col-0, *ltp2-1* and an *ltp1 ltp2* double knockdown. **H**. Representative images of toluidine blue stained hypocotyls from Col-0, *ltp2-1* and an *ltp1 ltp2* double mutant 7 days after stratification.

Figure S1. A. *LTP2* is induced in the dark. Shown is the relative expression of *LTP2* in light vs dark-grown shoots at 7d post-stratification. B. Boxplot of log10(counts+1) for 19,987 genes expressed in our RNA-seq dataset from dark-grown shoots at 7d post-stratification; the black dot indicates *LTP2*. In Col-0 wild type, *LTP2* was the 7th most highly expressed gene. **C**. Scatterplot of hypocotyl length vs orientation for each individual, measured at 7d post-stratification; little correlation was found; indicated is Spearman ρ and p-value.

Figure S2. A. Boxplots of hypocotyl length, at 7d post-stratification, for all 5 replicates from Figure 1, showing similar distributions. Replicates 1-3 are from different seed batches, replicates 4-5 are the same seed batch done on different days. **B**. (top) Time-dependent decrease in the Pearson correlation coefficient between hypocotyl and root length at 3, 4, 5 and 7d post-stratification. Values are similar for *ltp2* and Col-0 supporting similar timing and uniformity of germination in *ltp2*. **C**. Scatterplot of hypocotyl length vs seed area (arbitrary units), showing little correlation; indicated is the Spearman ρ and p-value.

Figure S3. A. Hypocotyl (top) and root length (bottom) as a function of time since stratification in Col-0 seedlings grown on MS (open circles) or MS+1%sucrose (filled circles). B. Boxplots comparing the distribution of individual hypocotyl/root ratios for Col-0 seedlings grown on MS (open circles) and MS+1%sucrose (filled circles). C. Boxplots of hypocotyl length for seedlings grown on MS+1% sucrose on either vertical plates (shoot in contact with the media) or horizontal plates (only the roots contact the media); shows that direct sucrose uptake from the shoot is involved in sucrose-induced hypocotyl elongation.

Figure S4. A. Similar numbers of reads (>40 Mio) were obtained for each of the 8 RNA-seq samples. **B**. Correlation matrix for all 8 x 8 sample comparisons; Pearson correlation coefficients between replicates are all > 0.98. **C**. Boxplots of log10(counts) for all 8 samples showing no major difference in count distributions between Col-0 and *ltp2*. **D**. (left) Venn-diagram showing the overlap in DEGs (black; 11) between *ltp2*-L vs *ltp2*-S and Col-L vs Col-S; (right) Fold-change and p-value for the 10 DEGs common to long x short comparisons in Col-0 and *ltp2*. **E**. Boxplot of log10(counts) for all 19,983 genes in our dataset; orange circles: 10

genes from (**D**). **F**. Distance in log10 of the number of DEGs plotted against distance in mean hypocotyl length for each of four sample pairwise-comparisons. **G**. Venn-diagram showing the overlap in DEGs (gray; 474) between the comparison *ltp2*-L vs *ltp2*-S and Col-S vs *ltp2*-S. H. GO term enrichments (fold-enrichment >= 2, p-adj < 0.05) for the set of DEGs unique to Col-S vs *ltp2*-S (1164; see **G**).

Figure S5. A. Tree depicting the aminoacid similarity between PR14/Type I LTP proteins. **B**. Plot shows all the Type I LTPs expressed in our RNA-seq dataset of dark-grown shoots (x-axis) and the contribution of each (in %; y-axis) to the subfamily total in these samples. For this analysis, the counts from all four Col-0 samples and all four *ltp2* samples were averaged.
C. Plot shows the gene expression rank of *LTP2* and *LTP1* relative to all 26,372 genes, across a curated dataset of 56 Arabidopsis RNA-seq samples (see Methods); samples are ordered from highest to lowest; open circle is *LTP1*; filled circle is *LTP2*. In 41 out of 56 samples *LTP1* was higher than *LTP2*, indicating that *LTP1* is the dominant paralog by expression level.
D. The *LTP1/LTP2* expression ratio is fairly constant across individuals, regardless of their hypocotyl length; shown is the relation between hypocotyl length (at 7d post-stratification) and the log10(*LTP1/LTP2*) expression ratio for individual shoots. **E**. The *LTP1/LTP2* expression ratio changes during development; dark-grown seedlings have the lowest ratio compared to all other tested samples (light-grown seedlings, roots, leaves and flowers).

Table S1-S4. Differential expressed genes between Col-L and Col-S (Table S1), *ltp2*-L and *ltp2*-S (Table S2), Col-L and *ltp2*-L (Table S3), Col-S and *ltp2*-L (Table S4).

Table S5. Differentially expressed auxin-responsive genes not shared between Col-S vs *ltp2*-S and *ltp2*-L vs *ltp2*-S.

Table S6. Cuticle-related genes from Li-Beisson et al., 2013 expressed in our RNA-seq dataset.

Table S7. List of primers used in genotyping and qRT-PCR.
Table S8. List of publicly available RNA-seq samples used to establish global expression patterns for *LTP1* and *LTP2*.

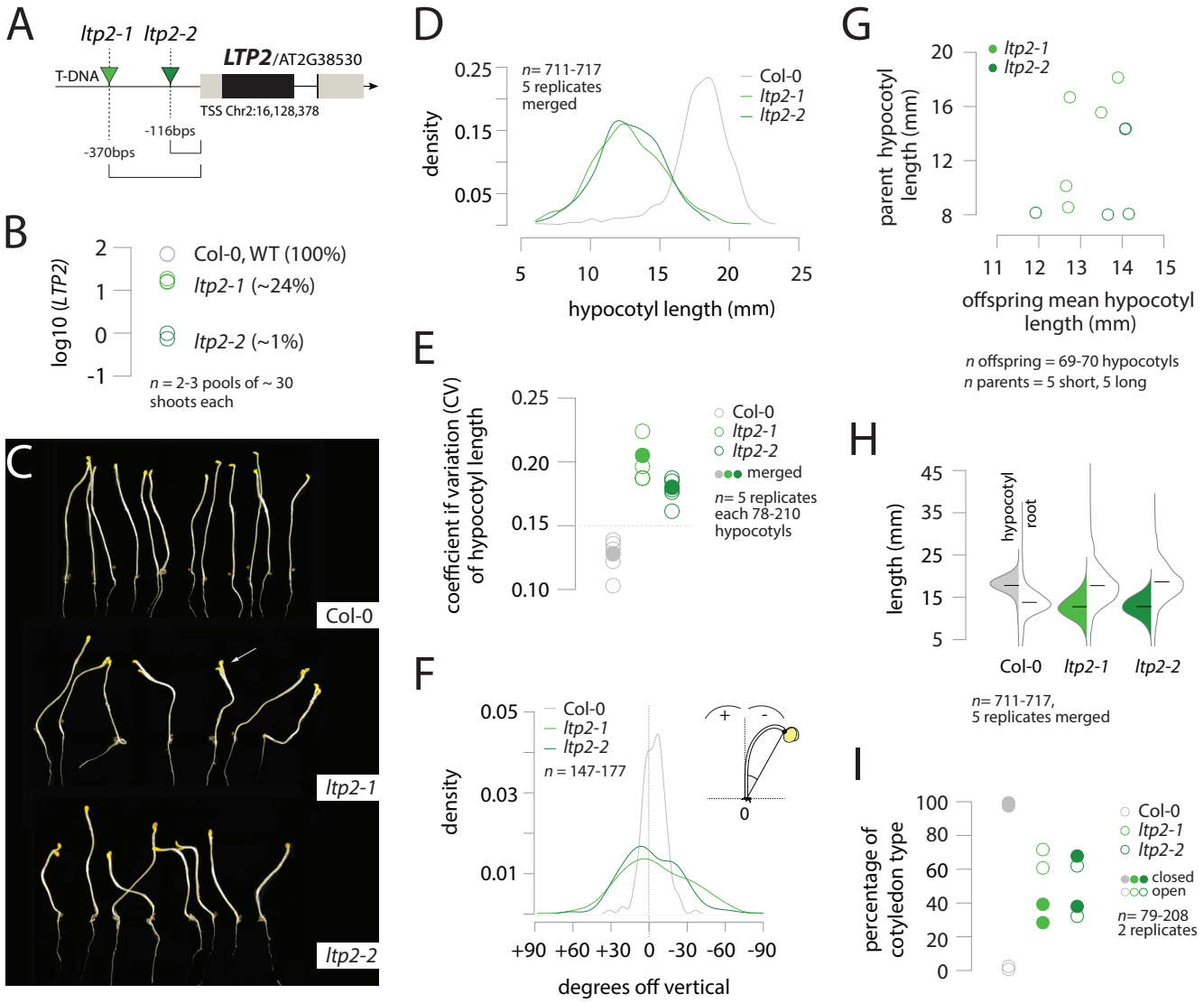
A
ltp2-1
ltp2-2
T-DNA
LTP2/AT2G38530
TSS Chr2:16,128,378
-116bps
-370bps
B
log10 (LTP2)
2
1
0
-1
Col-0, WT (100%)
ltp2-1 (~24%)
ltp2-2 (~1%)
n = 2-3 pools of ~ 30 shoots each
C
Col-0
ltp2-1
ltp2-2
D
density
0.25
0.15
0.05
n= 711-717
5 replicates merged
Col-0
ltp2-1
ltp2-2
5
10
15
20
25
hypocotyl length (mm)
E
coefficient if variation (CV) of hypocotyl length
0.25
0.20
0.15
0.10
Col-0
ltp2-1
ltp2-2
merged
n= 5 replicates each 78-210 hypocotyls
F
density
0.05
0.03
0.01
Col-0
ltp2-1
ltp2-2
n = 147-177
+
-
0
+90 +60 +30 0 -30 -60 -90
degrees off vertical
G
parent hypocotyl length (mm)
20
16
12
8
ltp2-1
ltp2-2
11 12 13 14 15
offspring mean hypocotyl length (mm)
n offspring = 69-70 hypocotyls
n parents = 5 short, 5 long
H
length (mm)
45
35
25
15
5
hypocotyl
root
Col-0
ltp2-1
ltp2-2
n= 711-717,
5 replicates merged
I
percentage of cotyledon type
100
80
60
40
20
0
Col-0
ltp2-1
ltp2-2
closed
open
n= 79-208
2 replicates

Figure 1

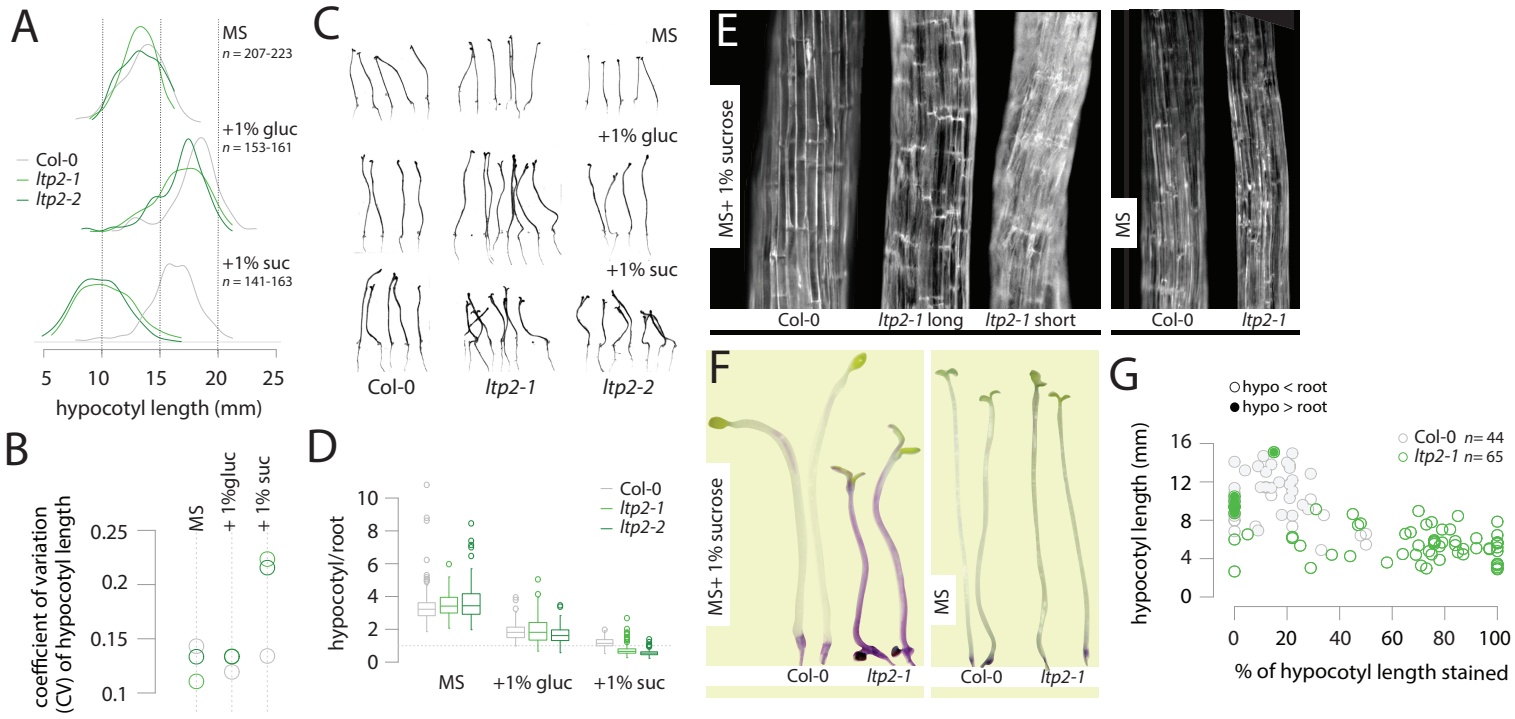
A
MS
n = 207-223
+1% gluc
n = 153-161
+1% suc
n = 141-163
Col-0
ltp2-1
ltp2-2
5
10
15
20
25
hypocotyl length (mm)
B
coefficient of variation (CV) of hypocotyl length
0.25
0.2
0.15
0.1
MS
+ 1%gluc
+ 1% suc
C
MS
+1% gluc
+1% suc
Col-0
ltp2-1
ltp2-2
D
hypocotyl/root
10
8
6
4
2
0
Col-0
ltp2-1
ltp2-2
MS
+1% gluc
+1% suc
E
MS+ 1% sucrose
Col-0
ltp2-1 long
ltp2-1 short
MS
Col-0
ltp2-1
F
MS+ 1% sucrose
Col-0
ltp2-1
MS
Col-0
ltp2-1
G
hypo < root
hypo > root
hypocotyl length (mm)
16
12
8
4
0
Col-0 n= 44
ltp2-1 n= 65
0
20
40
60
80
100
% of hypocotyl length stained

Figure 2

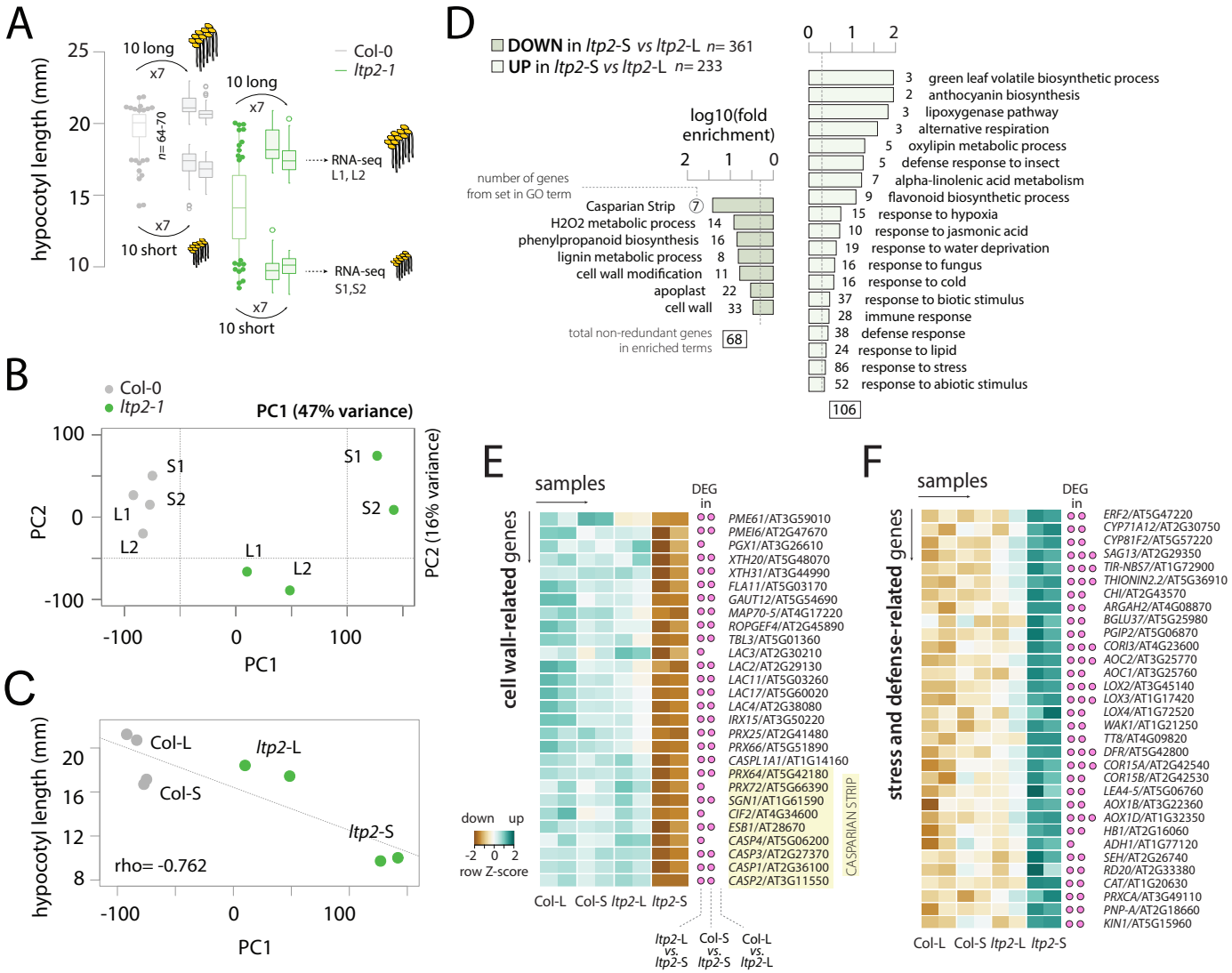
A
hypocotyl length (mm)
10 long
x7
10 short
n= 64-70
Col-0
ltp2-1
RNA-seq
L1, L2
RNA-seq
S1,S2
B
Col-0
ltp2-1
PC1 (47% variance)
PC2 (16% variance)
PC1
PC2
S1
S2
L1
L2
C
Col-L
Col-S
ltp2-L
ltp2-S
rho= -0.762
D
DOWN in ltp2-S vs ltp2-L n= 361
UP in ltp2-S vs ltp2-L n= 233
log10(fold enrichment)
number of genes from set in GO term
Casparian Strip 7
H2O2 metabolic process 14
phenylpropanoid biosynthesis 16
lignin metabolic process 8
cell wall modification 11
apoplast 22
cell wall 33
total non-redundant genes in enriched terms 68
3 green leaf volatile biosynthetic process
2 anthocyanin biosynthesis
3 lipoxygenase pathway
3 alternative respiration
5 oxylipin metabolic process
5 defense response to insect
7 alpha-linolenic acid metabolism
9 flavonoid biosynthetic process
15 response to hypoxia
10 response to jasmonic acid
19 response to water deprivation
16 response to fungus
16 response to cold
37 response to biotic stimulus
28 immune response
38 defense response
24 response to lipid
86 response to stress
52 response to abiotic stimulus
106
E
samples
DEG in
cell wall-related genes
PME61/AT3G59010
PMEI6/AT2G47670
PGX1/AT3G26610
XTH20/AT5G48070
XTH31/AT3G44990
FLA11/AT5G03170
GAUT12/AT5G54690
MAP70-5/AT4G17220
ROPGEF4/AT2G45890
TBL3/AT5G01360
LAC3/AT2G30210
LAC2/AT2G29130
LAC11/AT5G03260
LAC17/AT5G60020
LAC4/AT2G38080
IRX15/AT3G50220
PRX25/AT2G41480
PRX66/AT5G51890
CASPL1A1/AT1G14160
PRX64/AT5G42180
PRX72/AT5G66390
SGN1/AT1G61590
CIF2/AT4G34600
ESB1/AT28670
CASP4/AT5G06200
CASP3/AT2G27370
CASP1/AT2G36100
CASP2/AT3G11550
CASPARIAN STRIP
down up
row Z-score
Col-L Col-S ltp2-L ltp2-S
ltp2-L vs. ltp2-S
Col-S vs. ltp2-S
Col-L vs. ltp2-L
F
samples
DEG in
stress and defense-related genes
ERF2/AT5G47220
CYP71A12/AT2G30750
CYP81F2/AT5G57220
SAG13/AT2G29350
TIR-NBS7/AT1G72900
THIONIN2.2/AT5G36910
CHI/AT2G43570
ARGAH2/AT4G08870
BGLU37/AT5G25980
PGIP2/AT5G06870
CORI3/AT4G23600
AOC2/AT3G25770
AOC1/AT3G25760
LOX2/AT3G45140
LOX3/AT1G17420
LOX4/AT1G72520
WAK1/AT1G21250
TT8/AT4G09820
DFR/AT5G42800
COR15A/AT2G42540
COR15B/AT2G42530
LEA4-5/AT5G06760
AOX1B/AT3G22360
AOX1D/AT1G32350
HB1/AT2G16060
ADH1/AT1G77120
SEH/AT2G26740
RD20/AT2G33380
CAT/AT1G20630
PRXCA/AT3G49110
PNP-A/AT2G18660
KIN1/AT5G15960
Col-L Col-S ltp2-L ltp2-S

Figure 3

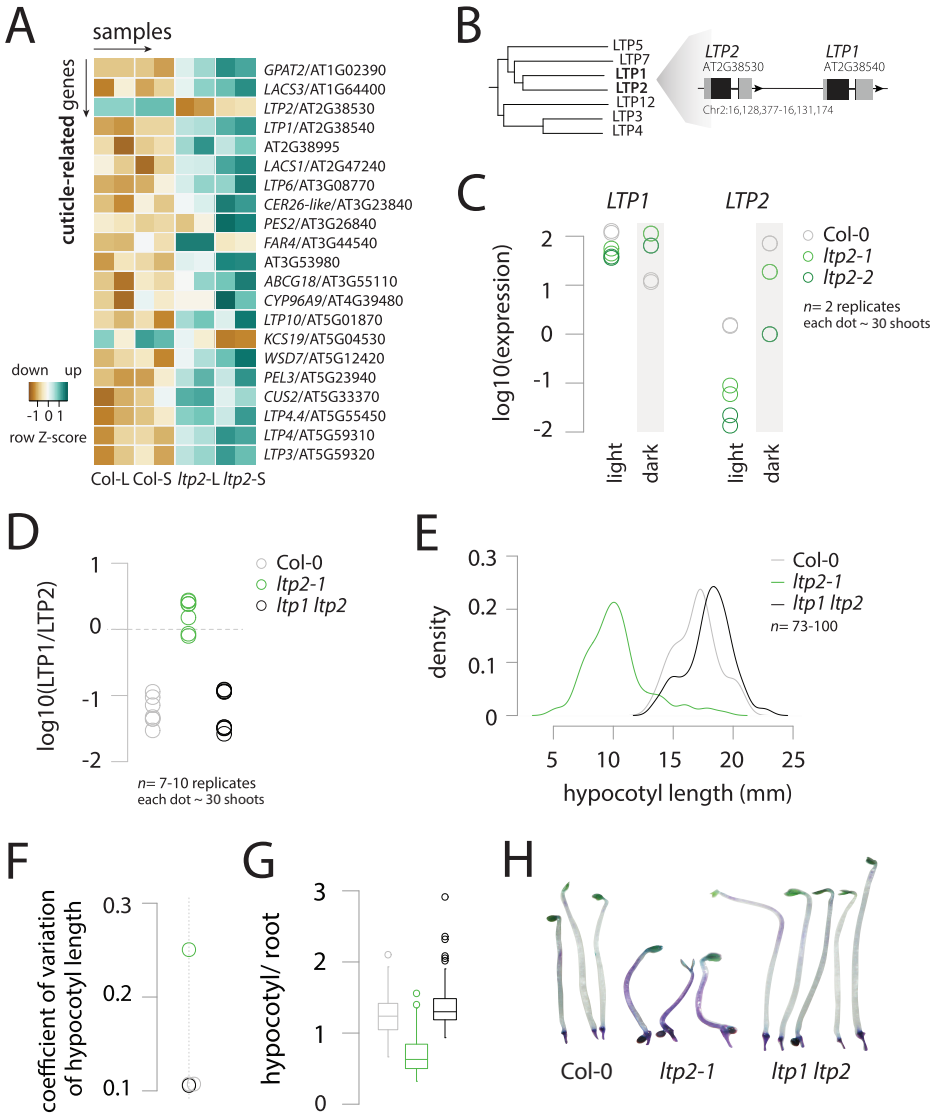
A
samples
cuticle-related genes
GPAT2/AT1G02390
LACS3/AT1G64400
LTP2/AT2G38530
LTP1/AT2G38540
AT2G38995
LACS1/AT2G47240
LTP6/AT3G08770
CER26-like/AT3G23840
PES2/AT3G26840
FAR4/AT3G44540
AT3G53980
ABCG18/AT3G55110
CYP96A9/AT4G39480
LTP10/AT5G01870
KCS19/AT5G04530
WSD7/AT5G12420
PEL3/AT5G23940
CUS2/AT5G33370
LTP4.4/AT5G55450
LTP4/AT5G59310
LTP3/AT5G59320
down up
-1 0 1
row Z-score
Col-L Col-S ltp2-L ltp2-S
B
LTP5
LTP7
LTP1
LTP2
LTP12
LTP3
LTP4
LTP2
AT2G38530
LTP1
AT2G38540
Chr2:16,128,377-16,131,174
C
LTP1
LTP2
log10(expression)
light
dark
light
dark
Col-0
ltp2-1
ltp2-2
n= 2 replicates
each dot ~ 30 shoots
D
log10(LTP1/LTP2)
Col-0
ltp2-1
ltp1 ltp2
n= 7-10 replicates
each dot ~ 30 shoots
E
density
Col-0
ltp2-1
ltp1 ltp2
n= 73-100
hypocotyl length (mm)
F
coefficient of variation
of hypocotyl length
G
hypocotyl/ root
H
Col-0
ltp2-1
ltp1 ltp2

Figure 4